Matrix Isolation Infrared Spectroscopic and Density Functional Theory Studies on the Reactions of Yttrium and Lanthanum Hydrides with Carbon Monoxide

Yun-Lei Teng and Qiang Xu*

National Institute of Advanced Industrial Science and Technology (AIST), Ikeda, Osaka 563-8577, Japan, and Graduate School of Engineering, Kobe University, Nada Ku, Kobe, Hyogo 657-8501, Japan

Received: July 31, 2007; In Final Form: October 7, 2007

Laser-ablated yttrium and lanthanum hydrides have been co-deposited at 4 K with carbon monoxide in excess argon. Products, such as HYCO, $(HY)_2CO$, HLaCO, $HLa(CO)_2$, and H_2LaCO, have been formed in the present experiments and characterized using infrared spectroscopy on the basis of the results of the isotopic shifts, mixed isotopic splitting patterns, stepwise annealing, the change of reagent concentration and laser energy, and the comparison with theoretical predictions. Density functional theory calculations have been performed on these molecules. The agreement between the experimental and calculated vibrational frequencies, relative absorption intensities, and isotopic shifts supports the identification of these molecules from the matrix infrared spectra. Plausible reaction mechanisms have been proposed to account for the formation of these molecules.

Introduction

The bonding of carbon monoxide with transition metals and transition-metal compounds is of great interest because of the importance of metal carbonyl species in a great many metal-catalyzed reactions involving CO.[1−3] The long-standing goal of elucidating mechanisms of the catalytic reactions involving CO has motivated numerous experimental and theoretical investigations of the interactions between metals and CO.[4] For example, the reactions of laser-ablated yttrium and lanthanum with carbon monoxide have been extensively studied, and products such as MCO (M = Y and La) and YCO^+ have been characterized.[5]

Metal hydrides are important as hydrogen storage materials for fuel cells.[6a] For instance, the $LaNi_5$ alloy has been found to reversibly absorb/desorb hydrogen.[6b,6c] The reactions of laser-ablated Sc, Y, and La with molecular hydrogen in excess argon have been reported, and the products MH, MH_2^+, MH_2, and MH_4^- (M = Sc, Y, and La) have been characterized by infrared spectroscopy.[7] On the other hand, a number of important metal-catalyzed reactions using syn-gas, such as methanol synthesis, oxo process, and Fischer−Tropsch synthesis, involve metal−carbonyl−hydride species as the reaction intermediates.[8a] There have been reports of metal−carbonyl−hydride complexes such as $HW(CO)_2$,[8b] $H_2M(CO)_4$ (M = Fe, Ru, Os), and $HCo(CO)_4$.[8c−8f] Such metal−carbonyl−hydride species may also play an important role in the degradation of anode catalyst of polymer electrolyte fuel cells (PEFCs) using hydrogen-containing CO impurity produced from steam reforming or the partial oxidation of alcohols or hydrocarbons.[9] As a rare example, the reactions of laser-ablated ruthenium atoms with carbon monoxide and hydrogen in solid argon have been recently investigated, and the products, such as the ruthenium carbonyl dihydride $H_2Ru(CO)_2$ and the hydrogen complexes $(H_2)_xRuCO$ (x = 1, 2), have been observed.[10]

Recent studies have shown that, with the aid of isotopic substitution techniques, matrix isolation infrared spectroscopy combined with quantum chemical calculation is very powerful for investigating the structure and bonding of novel species.[4,11,12] To understand the formation of carbonyl−hydride species of yttrium and lanthanum, the reactions of laser-ablated yttrium and lanthanum hydrides with carbon monoxide in a solid argon matrix have been performed. IR spectroscopy and theoretical calculations provide evidence for the formation of products, such as HYCO, $(HY)_2CO$, HLaCO, $HLa(CO)_2$, and H_2LaCO. To the best of our knowledge, this is the first example of the reactions of laser-ablated metal hydrides with small molecules in the field of matrix isolation infrared spectroscopy.

Experimental and Theoretical Methods. The experiment for laser ablation and matrix-isolation infrared spectroscopy is similar to those previously reported.[12] Briefly, the Nd:YAG laser fundamental (1064 nm, 10-Hz repetition rate with 10-ns pulse width) was focused on the rotating YH_2 (>99.9%, High Purity Chemicals) and LaH_x (>99%, High Purity Chemicals) targets. The laser-ablated species were co-deposited with CO in excess argon onto a CsI window cooled normally to 4 K by means of a closed-cycle helium refrigerator (V24SC6LSCP, Daikin Industries). Typically, a 3−30-mJ/pulse laser power was used. Carbon monoxide (99.95% CO), $^{13}C^{16}O$ (99%, ^{18}O < 1%), and $^{12}C^{18}O$ (99%) were used to prepare the CO/Ar mixtures. In general, matrix samples were deposited for 30−60 min with a typical rate of 2−4 mmol per hour. After sample deposition, IR spectra were recorded on a BIO-RAD FTS-6000e spectrometer at 0.5-cm^{-1} resolution using a liquid nitrogen cooled HgCdTe (MCT) detector for the spectral range of 5000−400 cm^{-1}. Samples were annealed at different temperatures and subjected to broad-band irradiation (λ > 250 nm) using a high-pressure mercury arc lamp (Ushio, 100 W).

Quantum chemical calculations were performed to predict the structures and vibrational frequencies of the observed reaction products using the Gaussian 03 program.[13] The B3LYP and B3PW91 density functional methods were utilized.[14] The 6-311++G(3df, 3pd) basis set was used for H, C, and O atoms, and SDD basis set was used for Y and La atoms.[15,16] The previous investigations have shown that such computational methods can provide reliable information for the Y- and La-containing molecules, such as infrared frequencies, relative

* To whom correspondence should be addressed. E-mail: q.xu@aist.go.jp.

10.1021/jp076053l CCC: $37.00
Published on Web 12/06/2007

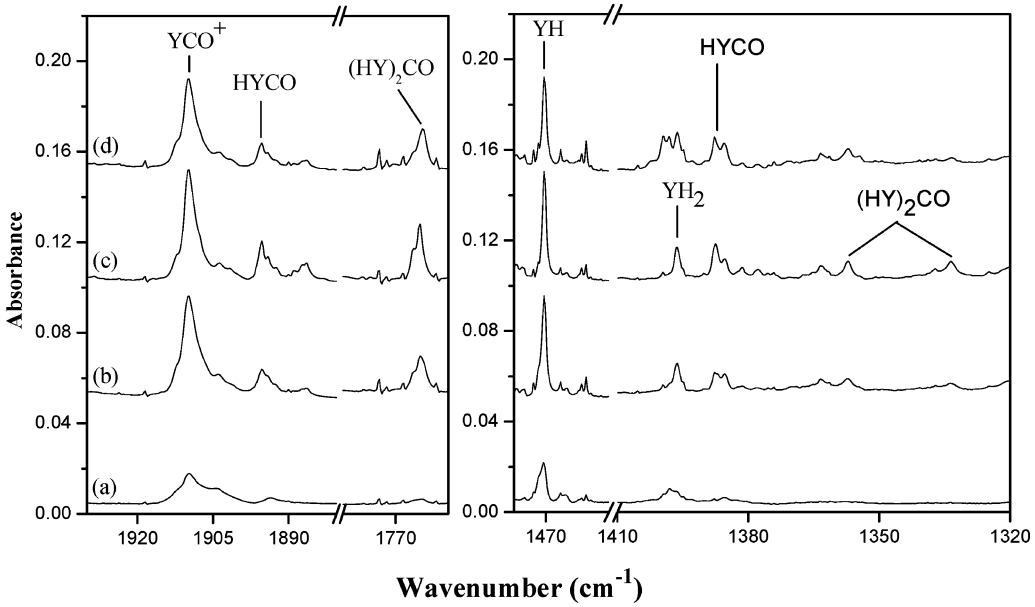

Figure 1. Infrared spectra in the 1930−1760- and 1480−1320-cm^{-1} regions from co-deposition of laser-ablated yttrium hydride with 0.04% CO in argon: (a) 1 h sample deposition at 4 K; (b) after annealing to 25 K; (c) after annealing to 30 K; (d) after 15 min of broad-band irradiation.

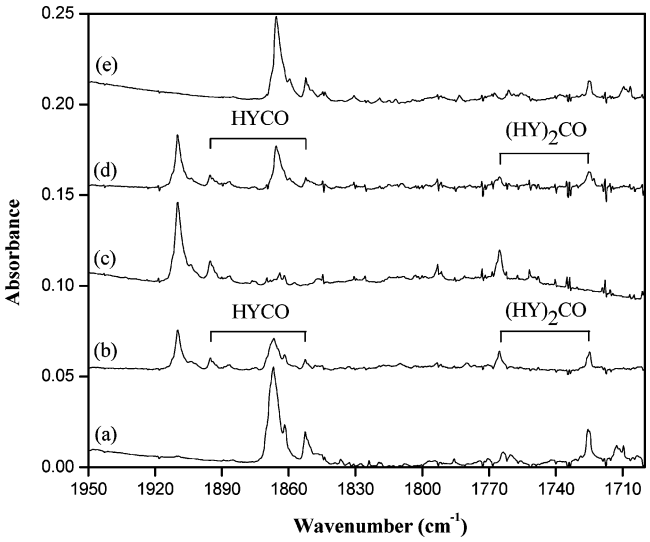

Figure 2. Infrared spectra in the 1950−1700-cm^{-1} region from co-deposition of laser-ablated yttrium hydride with CO in argon after annealing to 25 K: (a) 0.04% $^{13}C^{16}O$; (b) 0.02% $^{12}C^{16}O$ + 0.02% $^{13}C^{16}O$; (c) 0.04% $^{12}C^{16}O$; (d) 0.02% $^{12}C^{16}O$ + 0.02% $^{12}C^{18}O$; (e) 0.04% $^{12}C^{18}O$.

absorption intensities, and isotopic shifts.[5a,10] Geometries were fully optimized, and vibrational frequencies were calculated with analytical second derivatives.

Results and Discussion

Experiments have been done with CO concentrations ranging from 0.02 to 0.5% in excess argon. Typical infrared spectra for the reactions of laser-ablated YH_2 and LaH_x with CO in excess argon in the selected regions are illustrated in Figures 1−4, and the absorption bands are listed in Table 1. The stepwise annealing and irradiation behavior of these product absorptions are also shown in the figures and will be discussed below.

Quantum chemical calculations have been carried out for the possible isomers and electronic states of the potential product molecules. Figure 5 shows the optimized structures and electronic ground states. Table 2 reports a comparison of the observed and calculated IR frequencies and isotopic frequency ratios of the reaction products. Calculated vibrational frequencies and intensities of the potential products are listed in Table 3.

HYCO. Laser ablation of an YH_2 target gives rise to a strong IR absorption at 1470.5 cm^{-1} due to YH.[5] For the YH_2 + CO experiments, an intense absorption is observed at 1909.9 cm^{-1} for YCO^+,[5b] indicating that Y atoms are also produced during the laser ablation of YH_2. In addition to the absorptions due to yttrium carbonyls observed in the experiments of laser ablation of Y with CO and the yttrium hydrides observed in the experiments of laser ablation of YH_2, new absorptions at 1895.2, 1765.4, 1387.5, 1357.2, and 1333.6 cm^{-1} are observed in the experiments of laser ablation of YH_2 with CO. The absorptions at 1895.2 and 1387.5 cm^{-1} appear on sample deposition, visibly increase on sample annealing to 25 K, and further increase on annealing to 30 K (Table 1 and Figure 1). The 1895.2-cm^{-1} band shifts to 1852.6 cm^{-1} with $^{13}C^{16}O$ and to 1852.3 cm^{-1} with $^{12}C^{18}O$, exhibiting isotopic frequency ratios ($^{12}C^{16}O/^{13}C^{16}O$, 1.0230; $^{12}C^{16}O/^{12}C^{18}O$, 1.0232) characteristic of C−O stretching vibration. As shown in Figure 2, the mixed $^{12}C^{16}O$ + $^{13}C^{16}O$ and $^{12}C^{16}O$ + $^{12}C^{18}O$ isotopic spectra only provide the sum of pure isotopic bands, which indicates that only one CO subunit is involved in this mode. The absorptions at 1895.2 and 1387.5 cm^{-1} can be grouped together to one species, based on the growth/decay characteristics as a function of changes of experimental conditions. The position of the 1387.5-cm^{-1} band indicates a Y−H stretching vibration. Doping with CCl_4 has no effect on these bands, which suggests that the product is neutral. The 1895.2- and 1387.5-cm^{-1} bands are therefore assigned to the C−O and Y−H stretching vibrations of the neutral HYCO molecule, respectively.

B3LYP and B3PW91 calculations of three different geometric HYCO isomers with different electronic states, such as end-bonded HYCO, side-bonded HY-(η^2-CO), and isocarbonyl HYOC, have been performed. By use of the B3LYP calculated results as an example, all three of the HYCO isomers are predicted to be stable relative to the ground-state Y atom and CO molecule, and all have a triplet ground state. The end-bonded HYCO is the global minimum, which is 8.2 and 17.7 kcal/mol lower in energy than the HY-(η^2-CO) and HYOC isomers, respectively (Figure 5). Furthermore, the triplet HYCO lies 9.3 kcal/mol lower in energy than the singlet one. As shown

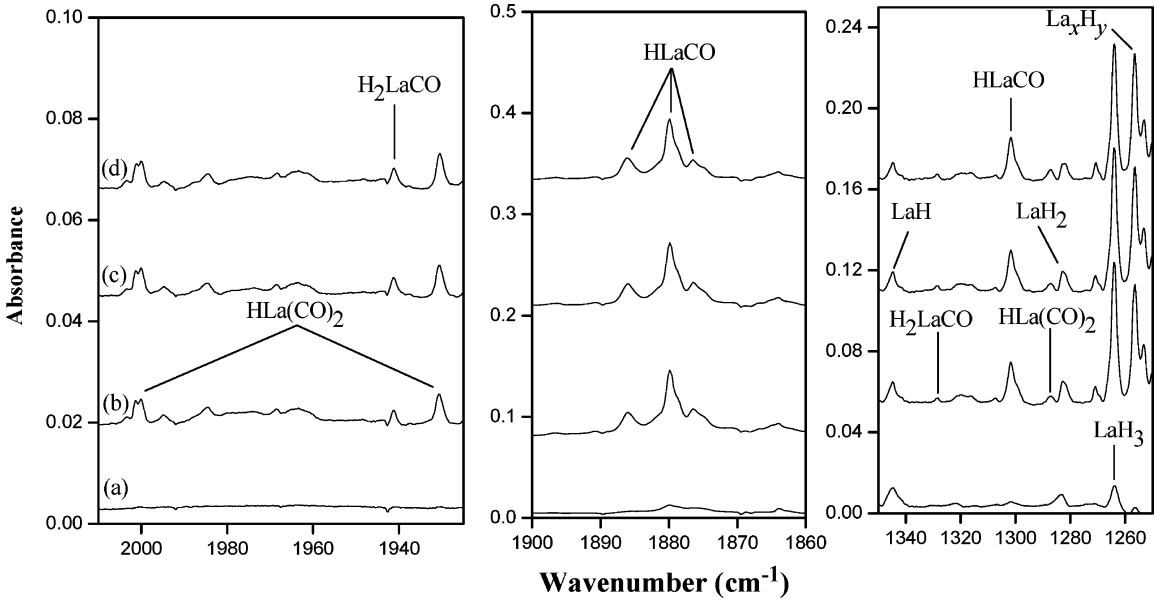

Figure 3. Infrared spectra in the 2010−1925-, 1900−1860-, and 1350−1275-cm^{-1} regions from co-deposition of laser-ablated lanthanum hydride with 0.1% CO in argon: (a) 1 h sample deposition at 4 K; (b) after annealing to 25 K; (c) after annealing to 30 K; (d) after annealing to 35 K.

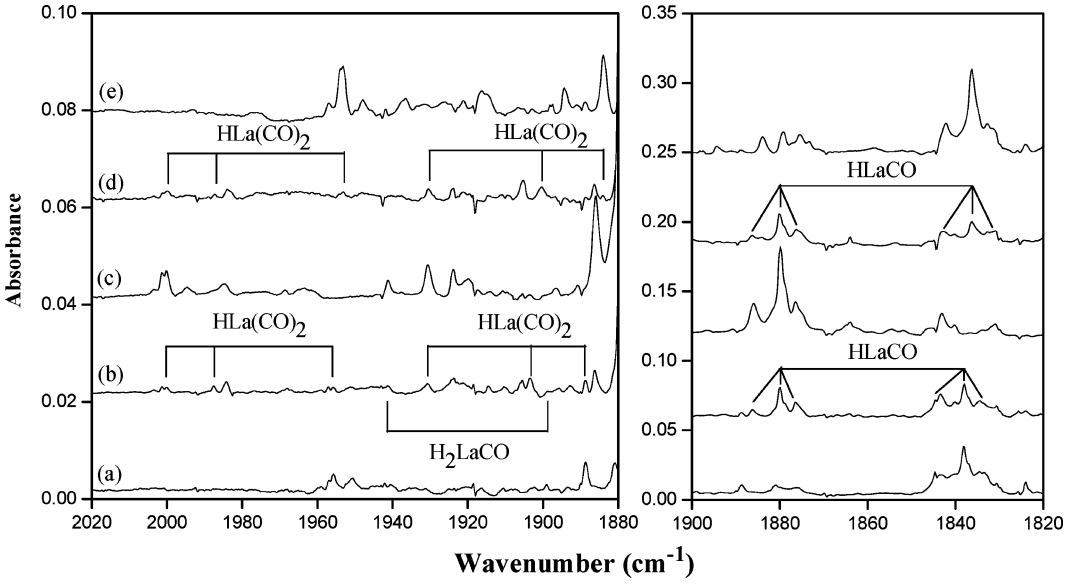

Figure 4. Infrared spectra in the 2020−1880- and 1900−1820-cm^{-1} regions from co-deposition of laser-ablated lanthanum hydride with CO in argon: (a) 0.1% $^{13}C^{16}O$; (b) 0.05% $^{12}C^{16}O$ + 0.05% $^{13}C^{16}O$; (c) 0.1% $^{12}C^{16}O$; (d) 0.06% $^{12}C^{16}O$ + 0.06% $^{12}C^{18}O$; (e) 0.1% $^{12}C^{18}O$.

in Table 2, the calculated C−O stretching and Y−H stretching vibrations for HYCO are 1956.8 and 1454.6 cm^{-1}, respectively, in agreement with the experimental observations (1895.2 and 1387.5 cm^{-1}). In contrast, the calculated C−O stretching vibrations for HY-(η^2-CO) and HYOC are 1686.6 and 1588.3 cm^{-1}, respectively, significantly lower than the observed value. The calculated $^{12}C^{16}O/^{13}C^{16}O$ and $^{12}C^{16}O/^{12}C^{18}O$ isotopic frequency ratios (1.0228 and 1.0245) for HYCO are also consistent with the experimental values (1.0230 and 1.0232).

$(HY)_2CO$. The absorption at 1765.4 cm^{-1} appears on sample deposition, visibly increases on sample annealing to 25 K, further increases on annealing to 30 K, and decreases on broad-band irradiation (Table 1 and Figure 1). The 1765.4-cm^{-1} band shifts to 1724.8 cm^{-1} with $^{13}C^{16}O$ and to 1724.7 cm^{-1} with $^{12}C^{18}O$, exhibiting isotopic frequency ratios ($^{12}C^{16}O/^{13}C^{16}O$, 1.0235; $^{12}C^{16}O/^{12}C^{18}O$, 1.0236) characteristic of C−O stretching vibration. As shown in Figure 2, in the mixed $^{12}C^{16}O$ + $^{13}C^{16}O$ and $^{12}C^{16}O$ + $^{12}C^{18}O$ experiments, only pure isotopic counterparts are observed, which indicates that only one CO subunit is involved in this mode. The 1357.2- and 1333.6-cm^{-1} bands track with the 1765.8 cm^{-1} bands, suggesting different modes of the same molecule. The positions of the 1357.2- and 1333.6-cm^{-1} bands indicate that they are due to Y−H stretching vibrations. Furthermore, these bands are favored with higher laser energy, indicating that more than one HY unit is involved. Doping with CCl_4 has no effect on these bands, suggesting that the product is neutral. These bands are therefore assigned to the neutral $(HY)_2CO$ molecule.

Our calculations predict that the $(HY)_2CO$ has a $^1A_1$ ground state with C_{2v} symmetry (Figure 5). The C−O and the symmetric and antisymmetric Y−H stretching vibrational frequencies are calculated at 1805.3, 1422.3, and 1405.3 cm^{-1} (Tables 2 and 3), which must be scaled down by 0.980, 0.954, and 0.950 to fit the experimental observations of 1765.4, 1357.2, and 1333.6 cm^{-1}, respectively. The calculated $^{12}C^{16}O/^{13}C^{16}O$ and $^{12}C^{16}O/^{12}C^{18}O$ isotopic frequency ratios are also consistent with the experimental observations. These agreements between the experimental and calculated vibrational frequencies, relative

TABLE 1: Infrared Absorptions (cm^{-1}) from Co-Deposition of Laser-Ablated YH_2 and LaH_x with CO in Excess Argon at 4 K

$^{12}C^{16}O$	$^{13}C^{16}O$	$^{12}C^{18}O$	$^{12}C^{16}O + {}^{13}C^{16}O$	$^{12}C^{16}O + {}^{12}C^{18}O$	*R*(12/13)	*R*(16/18)	assignment[a]
1895.2	1852.6	1852.3	1895.3, 1852.6	1895.3, 1852.3	1.0230	1.0232	HYCO, CO str.
1765.4	1724.8	1724.7	1765.4, 1724.8	1765.4, 1724.7	1.0235	1.0236	$(HY)_2CO$, CO str.
1387.5	1387.4	1387.3	1387.2	1387.3			HYCO, YH str.
1357.2	1357.1	1357.2	1357.3	1357.2			$(HY)_2CO$, s-YH str.
1333.6	1333.5	1333.6	1333.5	1333.5			$(HY)_2CO$, as-YH str.
2000.1	1955.7	1953.2	2000.1, 1987.7, 1955.8	2000.2, 1987.5, 1953.3	1.0227	1.0240	$HLa(CO)_2$, s-CO str.
1941.2	1899.3	1894.3	1940.9, 1898.8	1939.3, 1894.3	1.0221	1.0248	H_2LaCO, CO str.
1930.5	1888.7	1884.0	1930.7, 1903.5, 1888.7	1930.5, 1905.6, 1884.0	1.0221	1.0247	$HLa(CO)_2$, as-CO str.
1886.2	1843.2	1842.1	1886.2, 1843.5	1886.2, 1842.3	1.0233	1.0239	HLaCO site, CO str.
1880.0	1838.1	1836.2	1880.0, 1838.1	1879.8, 1836.2	1.0228	1.0239	HLaCO, CO str.
1876.3	1834.5	1831.0	1876.3, 1834.5	1876.3, 1831.0	1.0228	1.0247	HLaCO site, CO str.
1328.4	1328.3	1328.2	1328.4	1328.4			H_2LaCO, LaH s-str.
1301.7	1301.5	1301.5	1301.7	1301.6			HLaCO, LaH str.
1287.4	1287.3	1287.2	1286.9	1286.7			$HLa(CO)_2$, LaH str.

[a] s = symmetric, as = asymmetric, str. = stretching mode.

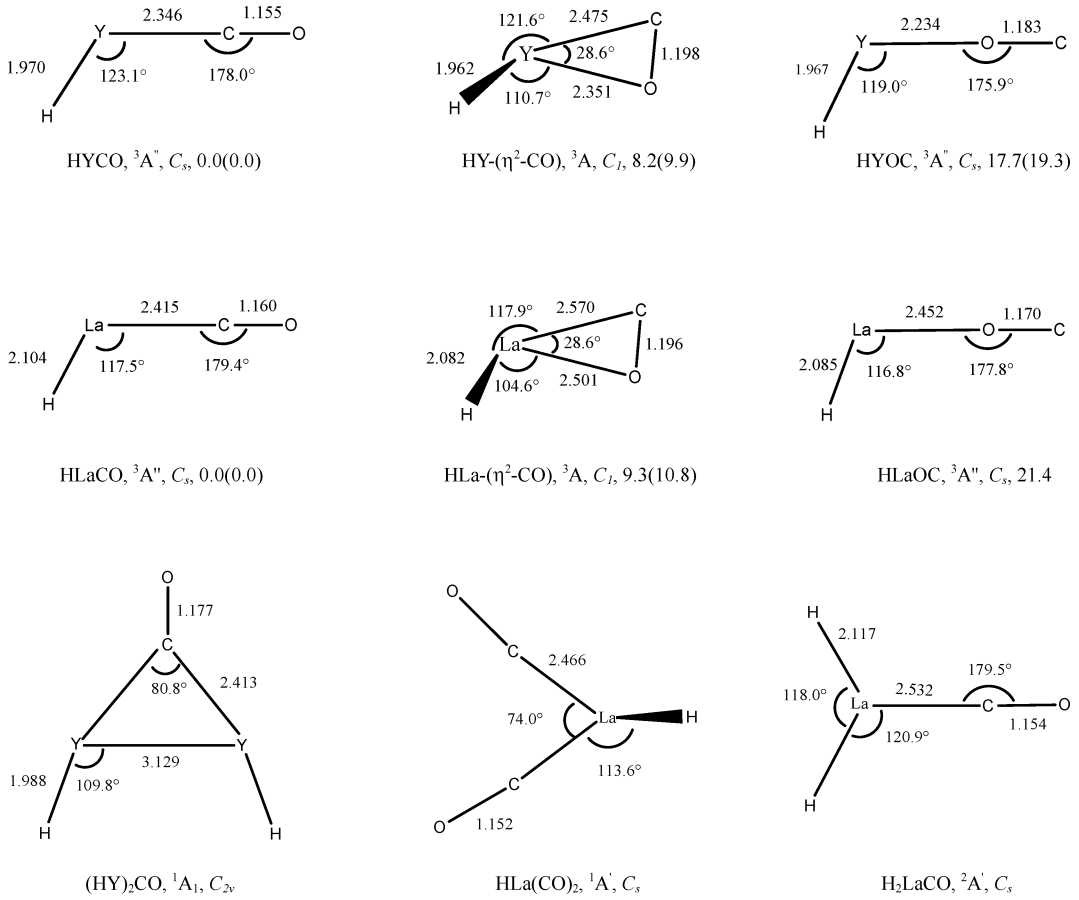

Figure 5. Optimized structures (bond length in angstroms, bond angle in degree), electronic ground states, and the relative energies (in kilocalories per mole) of the possible products and isomers calculated at the B3LYP/6-311++G(3df, 3pd)-SDD and B3PW91/6-311++G(3df, 3pd)-SDD (in parentheses) levels.

absorption intensities, and isotopic shifts confirm the identification of the $(HY)_2CO$ molecule from the matrix IR spectra.

HLaCO. Intense IR absorptions due to LaH (1345.2 cm^{-1}), LaH_2 (1282.9 and 1221.1 cm^{-1}), and LaH_3 (1263.9 cm^{-1}) are observed in the experiment of laser ablation of a LaH_x target, for which the IR absorptions are in agreement with the previous reported values.[5] For the LaH_x + CO experiments, an intense absorption is observed at 1773.3 cm^{-1} for LaCO,[5c] indicating that La atoms are also produced during the laser ablation of LaH_x. In addition to the absorptions due to lanthanum carbonyls observed in the experiments of laser ablation of La with CO and the lanthanum hydrides observed in the experiments of laser ablation of LaH_x, new absorptions at 2000.1, 1941.2, 1930.5, 1886.2, 1880.0, 1876.3, 1328.4, 1301.7, and 1287.4 cm^{-1} are observed in the experiments of laser ablation of LaH_x with CO. The absorption at 1880.0 cm^{-1} with two trapping sites at 1886.2 and 1876.3 cm^{-1} aappears during sample deposition, markedly increases on annealing to 25 K, and visibly increases on further annealing to 30 K (Table 1 and Figure 3). The 1880.0-cm^{-1} band shifts to 1838.1 cm^{-1} with $^{13}C^{16}O$ and to 1836.2 cm^{-1} with $^{12}C^{18}O$, exhibiting isotopic frequency ratios ($^{12}C^{16}O/^{13}C^{16}O$, 1.0228; $^{12}C^{16}O/^{12}C^{18}O$, 1.0239) characteristic of C−O stretching vibration. The mixed $^{12}C^{16}O$ + $^{13}C^{16}O$ and $^{12}C^{16}O$ + $^{12}C^{18}O$ isotopic spectra only provide the sum of pure isotopic bands (Figure 4), which indicates that only one CO subunit is involved in this mode. The absorption at 1301.7 cm^{-1} exhibits the same annealing behavior with the 1880.0-cm^{-1} band, suggesting that the two absorptions are due to the different modes of the same

TABLE 2: Comparison of Observed and Calculated IR Frequencies (cm^{-1}) and Isotopic Frequency Ratios of the Reaction Product

		experimental			calculated			
species	mode[a]	freq (cm^{-1})	*R*(12/ 13)	*R*(16/18)	method	freq (cm^{-1})	*R*(12/ 13)	*R*(16/18)
HYCO	CO str.	1895.2	1.0230	1.0232	B3LYP	1956.8	1.0228	1.0245
					B3PW91	1961.9	1.0228	1.0247
	YH str.	1387.5			B3LYP	1454.6		
					B3PW91	1455.5		
$(HY)_2CO$	CO str.	1765.4	1.0235	1.0236	B3LYP	1805.3	1.0225	1.0256
					B3PW91	1814.9	1.0225	1.0251
	s-YH str.	1357.2			B3LYP	1422.3		
					B3PW91	1426.5		
	as-YH str.	1333.6			B3LYP	1405.3		
					B3PW91	1409.7		
HLaCO	CO str.	1880.0	1.0228	1.0239	B3LYP	1868.5	1.0221	1.0255
					B3PW91	1863.1	1.0224	1.0252
	LaH str.	1301.7			B3LYP	1340.3		
					B3PW91	1339.5		
$HLa(CO)_2$	s-CO str.	2000.1	1.0227	1.0240	B3LYP	2010.3	1.0230	1.0244
					B3PW91	2021.6	1.0230	1.0242
	as-CO str.	1930.5	1.0221	1.0247	B3LYP	1926.5	1.0225	1.0251
					B3PW91	1934.9	1.0225	1.0250
	LaH str.	1287.4			B3LYP	1338.5		
					B3PW91	1320.9		
H_2LaCO	CO str.	1941.2	1.0221	1.0248	B3LYP	1972.5	1.0229	1.0244
					B3PW91	1986.0	1.0299	1.0314
	s-LaH str.	1328.4			B3LYP	1360.7		
					B3PW91	1357.9		

[a] s = symmetric, as = asymmetric, str. = stretching mode.

TABLE 3: Ground Electronic States, Point Groups, Vibrational Frequencies (cm^{-1}), and Intensities (km/mol) of the Reaction Products Calculated at the B3LYP/6-311++G(3df, 3pd)-SDD Level (Only the Frequencies above 400 cm^{-1} Are Listed)

species	electronic state	point group	frequency (intensity, mode)
CO	$^1\Sigma^+$	$C_{\infty v}$	2216.1 (80, Σ^+)
YH	$^1\Sigma^+$	$C_{\infty v}$	1534.8 (264, Σ^+)
LaH	$^1\Sigma^+$	$C_{\infty v}$	1406.0 (464, Σ^+)
LaH_2	$^2A_1$	C_{2v}	1321.4 (524, A_1), 1274.1 (879, B_2), 419.1 (179, A_1)
HYCO	$^3A''$	C_s	1956.7 (1330, A′), 1454.5 (493, A′)
$(HY)_2CO$	$^1A_1$	C_{2v}	1805.3 (756, A_1), 1422.3 (577, A_1), 1405.3 (283, B_2)
HLaCO	$^3A''$	C_s	1868.5 (2988, A′), 1340.3 (703, A′), 408.3 (104, A′)
$HLa(CO)_2$	$^1A'$	C_s	2010.3 (946, A′), 1926.5 (1519, A″), 1338.5 (806, A′), 445.9 (4.8, A′)
H_2LaCO	$^2A'$	C_s	1972.5 (999, A′), 1360.7 (678, A′), 1310.9 (1147, A″), 553.6 (192, A′)

molecule. The position of the 1301.7-cm^{-1} band indicates a La−H stretching vibration. Doping with CCl_4 has no effect on these bands, which suggests that the product is neutral. The 1880.0- and 1301.7-cm^{-1} bands are therefore assigned to the C−O and La−H stretching vibrations of the neutral HLaCO molecule, respectively.

The present calculations lend support for the assignment of HLaCO. The HLaCO molecule is predicted to have a $^3A''$ electronic ground state with C_s symmetry (Figure 5) and is the most stable structural isomer of HLaCO. At the B3LYP level of theory, the triplet HLaCO lies 12.0 and 63.5 kcal/mol lower in energy than the singlet and quintet ones, respectively. The HLa-(η^2-CO) and HLaOC isomers are, respectively, 9.3 and 21.4 kcal/mol higher in energy than the end-bonded one (Figure 5). The C−O and La−H stretching vibrations for HLaCO are calculated at 1868.5 and 1340.3 cm^{-1} (Tables 2 and 3), respectively, which supports the above assignment. In contrast, the calculated C−O stretching vibrations for HLa-(η^2-CO) and HLaOC are 1684.3 and 1656.2 cm^{-1}, respectively, significantly lower than the observed value. Furthermore, as shown in Table 2, the calculated isotopic frequency ratios for HLaCO are also consistent with the experimental values.

$HLa(CO)_2$. The absorptions at 2000.1 and 1930.5 cm^{-1} appear during sample deposition, visibly increase on annealing to 25 K, and then slightly increase on further annealing to 30 K (Table 1 and Figure 3). The two bands respectively shift to 1955.7 and 1888.7 cm^{-1} with $^{13}C^{16}O$ and to 1953.2 and 1884.0 cm^{-1} with $^{12}C^{18}O$, exhibiting isotopic frequency ratios ($^{12}C^{16}O/^{13}C^{16}O$, 1.0227 and 1.0221; $^{12}C^{16}O/^{12}C^{18}O$, 1.0240 and 1.0247) characteristic of C−O stretching vibration. The mixed isotopic spectra give two sets of triplet bands with approximate 1:2:1 relative intensities (Table 1, Figure 4), which indicates that two equivalent CO subunits are involved. The absorption at 1287.4 cm^{-1} exhibits the same annealing behavior with the 2000.1 and 1930.5 cm^{-1} bands, suggesting that these absorptions are due to the different modes of the same molecule. The position of the 1287.4-cm^{-1} band indicates a La−H stretching vibration. Doping with CCl_4 has no effect on these bands, suggesting that the product is neutral. Accordingly, these bands are assigned to the symmetric, antisymmetric C−O and La−H stretching modes of the $HLa(CO)_2$ molecule.

$HLa(CO)_2$ is predicted to have a $^1A'$ ground state with C_s symmetry, which lies 7.0 kcal/mol lower in energy than the C_{2v} one at the B3LYP level of theory (Figure 5). The symmetric and antisymmetric C−O stretching and La−H stretching vibrational frequencies of $HLa(CO)_2$ are calculated at 2010.3, 1926.5, and 1338.5 cm^{-1} (Tables 2 and 3), which are in accord with our observed values, 2000.1, 1930.5, and 1287.4 cm^{-1}. As listed in Table 2, for the 2000.1-cm^{-1} band, the calculated $^{12}C^{16}O/^{13}C^{16}O$ and $^{12}C^{16}O/^{12}C^{18}O$ isotopic frequency ratios

(1.0230 and 1.0244) are consistent with the experimental observations (1.0227 and 1.0240). For the 1930.5-cm^{-1} band, the calculated $^{12}C^{16}O/^{13}C^{16}O$ and $^{12}C^{16}O/^{12}C^{18}O$ isotopic frequency ratios (1.0225 and 1.0251) are also consistent with the experimental observations (1.0221 and 1.0247). The assignment of the $HLa(CO)_2$ molecule is supported by these agreements between the experimental and calculated vibrational frequencies, relative absorption intensities, and isotopic shifts.

H_2LaCO. The absorption at 1941.2 cm^{-1} appears during sample deposition, markedly increases on annealing to 25 K, and visibly increases on further annealing to 30 K (Table 1 and Figure 3). This band shifts to 1899.3 cm^{-1} with $^{13}C^{16}O$ and to 1894.3 cm^{-1} with $^{12}C^{18}O$. The isotopic frequency ratios ($^{12}C^{16}O/^{13}C^{16}O = 1.0221$, $^{12}C^{16}O/^{12}C^{18}O = 1.0248$) indicate that the band is due to a C−O stretching vibration. Only the pure isotopic counterparts were observed in the mixed $^{12}C^{16}O + ^{13}C^{16}O$ and $^{12}C^{16}O + ^{12}C^{18}O$ experiments, which indicates that only one CO subunit is involved in this mode. An absorption at 1328.4 cm^{-1} exhibits the same annealing behavior with the 1941.2-cm^{-1} band, suggesting that the two absorptions are due to the different modes of the same molecule. The position of the 1328.4-cm^{-1} band suggests that this band is due to a La−H stretching vibration. Doping with CCl_4 has no effect on these bands, suggesting that the product is neutral. Accordingly, the 1941.2- and 1328.4-cm^{-1} bands are assigned to the H_2LaCO molecule.

The H_2LaCO molecule is predicted to have a $^2A'$ ground state with C_s symmetry. The C−O stretching vibrational frequencies of H_2LaCO are predicted at 1972.5 cm^{-1}, which should be multiplied by 0.9841 to fit the experimental observation (1941.2 cm^{-1}). The calculated $^{12}C^{16}O/^{13}C^{16}O$ and $^{12}C^{16}O/^{12}C^{18}O$ isotopic frequency ratios agree with the experimental ratios. The symmetric and antisymmetric La−H stretching vibrational frequencies are calculated at 1360.7 and 1310.9 cm^{-1} (Table 3). The observed 1328.4-cm^{-1} band is assigned to the symmetric La−H stretching vibration. The antisymmetric La−H stretching vibration may be covered by the absorptions of LaH_3 or La_xH_y.

Reaction Mechanism. On the basis of the behavior of sample annealing together with the observed species and calculated stable isomers, plausible reaction mechanisms can be proposed as follows. Laser ablation of an YH_2 target produces YH species, which are co-deposited with CO to form the HYCO and $(HY)_2CO$ complexes during sample deposition (Figure 1). These species markedly increase on annealing, suggesting that the ground state YH can react with carbon monoxide molecules to form the HYCO and $(HY)_2CO$ complexes spontaneously according to reactions 1 and 2, which are predicted to be exothermic by 13.5 and 36.5 kcal/mol, respectively.

$$YH\ (^1\Sigma^+) + CO\ (^1\Sigma^+) \rightarrow HYCO\ (^3A'') \qquad \Delta E = -13.5\ \text{kcal/mol} \quad (1)$$

$$2YH\ (^1\Sigma^+) + CO\ (^1\Sigma^+) \rightarrow (HY)_2CO\ (^1A_1) \qquad \Delta E = -36.5\ \text{kcal/mol} \quad (2)$$

LaH, LaH_2, and LaH_3 are produced in the experiment of laser ablation of a LaH_x target. Laser-ablated LaH co-deposits with carbon monoxide molecules to form the HLaCO and $HLa(CO)_2$ complexes during sample deposition (Figure 3), which markedly increase on annealing, suggesting that the ground state LaH can react with carbon monoxide molecules to form the HLaCO and $HLa(CO)_2$ complexes spontaneously according to reactions 3 and 4, which are predicted to be exothermic by 24.1 and 44.0 kcal/mol, respectively. The absorption of H_2LaCO markedly increases on annealing, suggesting that the ground state LaH_2 can also react with carbon monoxide molecules to form the H_2-LaCO complex spontaneously according to reaction 5, which is predicted to be exothermic by 21.5 kcal/mol.

$$LaH\ (^1\Sigma^+) + CO\ (^1\Sigma^+) \rightarrow HLaCO\ (^3A'') \qquad \Delta E = -24.1\ \text{kcal/mol} \quad (3)$$

$$LaH\ (^1\Sigma^+) + 2CO\ (^1\Sigma^+) \rightarrow HLa(CO)_2\ (^1A_1) \qquad \Delta E = -44.0\ \text{kcal/mol} \quad (4)$$

$$LaH_2\ (^2A_1) + CO\ (^1\Sigma^+) \rightarrow H_2LaCO\ (^2A') \qquad \Delta E = -21.5\ \text{kcal/mol} \quad (5)$$

Conclusions

Reactions of laser-ablated yttrium and lanthanum hydrides with carbon monoxide in excess argon have been studied using matrix-isolation infrared spectroscopy. On the basis of the isotopic shifts and splitting patterns, the HYCO, $(HY)_2CO$, HLaCO, $HLa(CO)_2$, and H_2LaCO molecules have been characterized. Density functional theory calculations have been performed, which lend strong support to the experimental assignments of the infrared spectra. In addition, the plausible reaction mechanism for the formation of the products has been proposed.

Acknowledgment. This work was supported by a Grant-in-Aid for Scientific Research (B) (Grant No. 17350012) from the Ministry of Education, Culture, Sports, Science and Technology (MEXT) of Japan. Y.-L.T. thanks JASSO and Kobe University for an Honors Scholarship.

References and Notes

(1) Cotton, F. A.; Wilkinson, G.; Murillo, C. A.; Bochmann, M. *Advanced Inorganic Chemistry*, 6th ed.; Wiley: New York, 1999.
(2) Muetterties, E. L.; Stein, J. *Chem. Rev.* **1979**, *79*, 479.
(3) Tumas, W.; Gitlin, B.; Rosan, A. M.; Yardley, J. T. *J. Am. Chem. Soc.* **1982**, *104*, 55.
(4) Zhou, M. F.; Andrews, L.; Bauschlicher, C. W., Jr. *Chem. Rev.* **2001**, *101*, 1931.
(5) (a) Jiang, L.; Xu, Q. *J. Phys. Chem. A* **2006**, *110*, 5636. (b) Zhou, M. F.; Andrews, L. *J. Phys. Chem. A* **1999**, *103*, 2964. (c) Xu, Q.; Jiang, L.; Zhou, R. Q. *Chem.−Eur. J.* **2006**, *12*, 3226.
(6) (a) Schlapbach, L.; Zuttel, A. *Nature (London)* **2001**, *414*, 353. (b) Percheron-Guégan, A.; Lartigue, C.; Achard, J. C. *J. Less-Common Met.* **1985**, *109*, 287. (c) Van Vucht, J. H. N.; Kuijpers, F. A.; Bruning, H. C. A. M. *Philips Res. Rep.* **1970**, *25*, 133.
(7) (a) Wang, X. F.; Chertihin, G. V.; Andrews, L. *J. Phys. Chem. A* **2002**, *106*, 9213. (b) Andrews, L. *Chem. Soc. Rev.* **2004**, *33*, 123.
(8) (a) Falbe, J., Es. *New Syntheses with Carbon Monoxide*; Springer-Verlag: Berlin, 1980. (b) Mahmoud, K. A.; Rest, A. J.; Alt, H. G. *Dalton Trans.* **1984**, 187. (c) Jonas, V.; Thiel, W. *J. Chem. Phys.* **1996**, *105*, 3636. (d) Bor, G. *Inorg. Chim. Acta* **1967**, *1*, 81. (f) Sweany, R. L. *J. Am. Chem. Soc.* **1982**, *104*, 3739.
(9) (a) Barbir, F. In *Handbook of Fuel Cells-Fundamental Technology and Applications*; Vielstich, W., Lamm, A., Gasteiger, H. A, Eds.; Wiley: Chichester, 2003; vol. 4. (b) Oetjen, H. F.; Schmidt, V. M.; Stimming, U.; Trila, F. *J. Electrochem. Soc.* **1996**, *143*, 3838. (c) Niedrach, L.; Mckee, D.; Paynter, J.; Danzig, I. *Electrochem. Technol.* **1967**, *5*, 318. (d) Watanabe, M.; Motoo, S. *J. Electroanal. Chem.* **1975**, *60*, 275. (e) Gasteiger, H. A.; Markovic, N.; Ross, P. N.; Cairns, E. J. *J. Phys. Chem.* **1994**, *98*, 617.
(10) Wang, X. F.; Andrews, L. *J. Phys. Chem. A* **2000**, *104*, 9892.
(11) (a) Himmel, H. J.; Downs, A. J.; Greene, T. M. *Chem. Rev.* **2002**, *102*, 4191 and references therein.
(12) (a) Burkholder, T. R.; Andrews, L. *J. Chem. Phys.* **1991**, *95*, 8697. (b) Zhou, M. F.; Tsumori, N.; Andrews, L.; Xu, Q. *J. Phys. Chem. A* **2003**, *107*, 2458. (c) Jiang, L.; Xu, Q. *J. Chem. Phys.* **2005**, *122*, 034505. (d) Jiang, L.; Xu, Q. *J. Am. Chem. Soc.* **2005**, *127*, 42. (e) Jiang, L.; Xu, Q. *J. Am. Chem. Soc.* **2005**, *127*, 8906. (f) Xu, Q.; Jiang, L.; Tsumori, N. *Angew. Chem., Int. Ed.* **2005**, *44*, 4338. (f) Jiang, L.; Teng, Y. L.; Xu, Q. *J. Phys. Chem. A* **2006**, *110*, 7092.
(13) Frisch, M. J.; Trucks, G. W.; Schlegel, H. B.; Scuseria, G. E.; Robb, M. A.; Cheeseman, J. R.; Montgomery, J. A., Jr.; Vreven, T.; Kudin, K. N.; Burant, J. C.; Millam, J. M.; Iyengar, S. S.; Tomasi, J.; Barone, V.;

Mennucci, B.; Cossi, M.; Scalmani, G.; Rega, N.; Petersson, G. A.; Nakatsuji, H.; Hada, M.; Ehara, M.; Toyota, K.; Fukuda, R.; Hasegawa, J.; Ishida, M.; Nakajima, T.; Honda, Y.; Kitao, O.; Nakai, H.; Klene, M.; Li, X.; Knox, J. E.; Hratchian, H. P.; Cross, J. B.; Adamo, C.; Jaramillo, J.; Gomperts, R.; Stratmann, R. E.; Yazyev, O.; Austin, A. J.; Cammi, R.; Pomelli, C.; Ochterski, J. W.; Ayala, P. Y.; Morokuma, K.; Voth, G. A.; Salvador, P.; Dannenberg, J. J.; Zakrzewski, V. G.; Dapprich, S.; Daniels, A. D.; Strain, M. C.; Farkas, O.; Malick, D. K.; Rabuck, A. D.; Raghavachari, K.; Foresman, J. B.; Ortiz, J. V.; Cui, Q.; Baboul, A. G.; Clifford, S.; Cioslowski, J.; Stefanov, B. B.; Liu, G.; Liashenko, A.; Piskorz, P.; Komaromi, I.; Martin, R. L.; Fox, D. J.; Keith, T.; Al-Laham, M. A.; Peng, C. Y.; Nanayakkara, A.; Challacombe, M.; Gill, P. M. W.; Johnson, B.; Chen, W.; Wong, M. W.; Gonzalez, C.; Pople, J. A. *Gaussian 03*, revision B.04; Gaussian, Inc.: Pittsburgh, PA 2003.

(14) (a) Lee, C.; Yang, E.; Parr, R. G. *Phys. Rev. B* **1988**, *37*, 785. (b) Becke, A. D. *J. Chem. Phys.* **1993**, *98*, 5648.

(15) (a) Krishnan, R.; Binkley, J. S.; Seeger, R.; Pople, J. A. *J. Chem. Phys.* **1980**, *72*, 650. (b) Frisch, M. J.; Pople, J. A.; Binkley, J. S. *J. Chem. Phys.* **1984**, *80*, 3265.

(16) Dolg, M.; Stoll, H.; Preuss, H. *J. Chem. Phys.* **1989**, *90*, 1730.